Journal of Science: Advanced Materials and Devices 9 (2024) 100715

Contents lists available at ScienceDirect

Journal of Science: Advanced Materials and Devices

journal homepage: www.elsevier.com/locate/jsamd

# Electrical circuit modeling for the relaxor response of bismuth magnesium tantalate pyrochlore

P.Y. Tan [a], K.B. Tan [a,*], C.C. Khaw [b], H.C. Ananda Murthy [c], R. Balachandran [d], S.K. Chen [e], O.J. Lee [f], K.Y. Chan [g], M. Lu [h]

[a] Department of Chemistry, Faculty of Science, Universiti Putra Malaysia, 43400, UPM, Serdang, Selangor, Malaysia
[b] Department of Mechanical and Material Engineering, Lee Kong Chian Faculty of Engineering and Science, Universiti Tunku Abdul Rahman, 43000 Bandar Sungai Long, Kajang, Selangor, Malaysia
[c] Department of Prosthodontics, Saveetha Dental College & Hospital, Saveetha Institute of Medical and Technical Science (SIMATS), Saveetha University, Chennai 600077, Tamil Nadu, India
[d] Department of Electronics and Communication Engineering, Adama Science and Technology University, Adama, P.O. Box:1888, Ethiopia
[e] Department of Physics, Faculty of Science, Universiti Putra Malaysia, 43400, UPM, Serdang, Selangor, Malaysia
[f] Faculty of Science and Marine Environment, Universiti Malaysia Terengganu, 21030, Kuala Nerus, Terengganu, Malaysia
[g] Centre for Advanced Devices and Systems, Faculty of Engineering, Multimedia University, Persiaran Multimedia, 63100, Cyberjaya, Selangor, Malaysia
[h] Key Laboratory of Functional Materials Physics and Chemistry of the Ministry of Education, The Joint Laboratory of MXene Materials, Jilin Normal University, Changchun, 130103, Jilin, PR China

ARTICLE INFO

*Keywords:*
Pyrochlore
Ac impedance
Relaxor
Dielectric
Equivalent circuit

ABSTRACT

The electrical properties of bismuth magnesium tantalate pyrochlore, $Bi_{3.30}Mg_{1.88}Ta_{2.82}O_{13.88}$ (BMT) were investigated by both inductor-capacitor-resistor (LCR) and impedance spectroscopy techniques covering a broad temperature range of 10–1073 K and a frequency range of 5 Hz - 1 MHz. At below ~180 K, BMT pyrochlore exhibited interesting relaxor behaviour that showed high dispersion characteristics in its frequency-temperature dependent dielectric constants, $\varepsilon'$ and dielectric losses, tan δ, respectively. The maximum $\varepsilon'_{max}$ of ~77 was obtained at the temperature maximum, $T_m$ of 154 K. The frequency-independent $\varepsilon'$ data above 154 K at a fixed frequency of 1 MHz can be well fitted with the Curie-Weiss law and the relaxation features of $Bi_{3.30}Mg_{1.88}Ta_{2.82}O_{13.88}$ obeyed the Vogel-Fulcher equation. The dielectric properties of $Bi_{3.30}Mg_{1.88}Ta_{2.82}O_{13.88}$ relaxor in the low temperature range of 20–320 K could be satisfactorily modeled with different equivalent circuits. In this perspective, a master circuit consisting of a parallel R-C-CPE element in series with a capacitor was required to accurately fit the low temperature data.

## 1. Introduction

Bismuth pyrochlores have excellent dielectric properties, which are suitably applied in a wide variety of applications, e.g., high frequency microwave filters, multilayer capacitors, supercapacitors and others [1–8]. One example of extensively studied pyrochlores is bismuth zinc niobate (BZN) with the general formula of $(Bi_{1.5}Zn_{0.5})(Zn_{0.5}Nb_{1.5})O_7$. BZN pyrochlore showed relaxor behaviour at cryogenic conditions with frequency-dependent $\varepsilon'$ at below ~180 K and then a frequency-independent $\varepsilon'$ of ~130 above ~180 K over the frequency range of $10^3$–$10^6$ Hz [4]. On the other hand, Ti doped BZN pyrochlore with the formula of $(Bi_{1.5}Zn_{0.5})(Nb_{0.5}Ti_{1.5})O_7$ (BZNT) also revealed relaxor-like response whose frequency-independent ε' was ~160 at above ~120 K over the similar frequency range. Such characteristics could be well modelled and fitted by equivalent circuits of various elements, including a parallel resistor (R), and capacitor (C), as well as with the inclusion of a constant phase element (CPE). The circuit modeling technique is particularly useful to gain further insights into the electrical behavior of the functional ceramics especially to understand the origin of the conduction mechanism involved [4,5].

A structurally related Ta pyrochlore analogue was found to have similar relaxor behaviour. BZT pyrochlore with the composition, $(Bi_{1.5}Zn_{0.5})(Zn_{0.5}Ta_{1.5})O_7$ (BZT) showed dielectric relaxation and a relatively lower $\varepsilon'$ of ~60 in the frequency range of $10^2$–$10^{10}$ Hz. The

Peer review under responsibility of Vietnam National University, Hanoi.
* Corresponding author.
*E-mail address:* tankarban@upm.edu.my (K.B. Tan).

https://doi.org/10.1016/j.jsamd.2024.100715
Received 15 November 2023; Received in revised form 21 March 2024; Accepted 1 April 2024
Available online 2 April 2024

dielectric relaxation of BZT pyrochlore could be attributed to the hopping of cations from the eight-coordinated A site, e.g., Zn/Bi with more than one equivalent potential minima [6,7]. This may also due to the reorientation of the dipoles that formed from the interactions between the A cations with the "seventh oxygen", i.e. O′ or O(2) within the $A_2B_2O_6O'$ pyrochlore structure [4–6]. In the case of Mg pyrochlore analogue, the reported $Bi_{1.667}Mg_{0.70}Nb_{1.52}O_7$ also demonstrated an interesting relaxation behaviour at sub-ambient temperature [7]. This agreed well with our reported study wherein BMN pyrochlore, e.g., $Bi_{3.55}Mg_{1.78}Nb_{2.67}O_{13.78}$ had a high $\varepsilon'_{max}$ of 209 at the $T_m$ of 204 K. The low temperature electrical data of BMN pyrochlore could be modelled accurately with suitable equivalent circuits that contained a parallel R-C-CPE element in series with a capacitor [2].

Considering the inconsistencies and discrepancies over the limited literature on the pyrochlores in $Bi_2O_3$–MgO–$Ta_2O_5$ (BMT) ternary system [2,3,8], their low temperature electrical behaviours are in particular yet to be fully characterised. Hence, we undertake careful electrical measurements and circuit fittings of BMT pyrochlore in consonance with several objectives below: (i) to characterise the low temperature electrical properties of BMT pyrochlore at different frequencies (ii) to fit the impedance data with various equivalent electrical circuits and (iii) to provide a physical interpretation of the electrical data using the proposed circuit models.

## 2. Experimental

Pyrochlore of the composition, $Bi_{3.30}Mg_{1.88}Ta_{2.82}O_{13.88}$ was prepared by conventional solid-state reaction. The pre-treated reagent grade oxide powders, $Bi_2O_3$ (Alfa Aesar, 99.99%), MgO (Aldrich, 99%) and $Ta_2O_5$ (Alfa Aesar, 99.9%) were used as the starting materials. The constituent oxides were weighed out in a proper ratio and were mixed homogeneously with acetone in an agate mortar. The mixed powders were then transferred into a platinum boat for calcination. The sample was fired at 300 °C and 600 °C, both for 1 h to ensure $Bi_2O_3$ had reacted to form less-volatile intermediates. This allowed subsequent firing at higher temperatures without significant bismuth losses. The powder was then heated at 800 °C overnight and followed by 1025 °C for 2–3 days with intermediate regrinding. Single phase $Bi_{3.30}Mg_{1.88}Ta_{2.82}O_{13.88}$ was confirmed by an automated Shimadzu diffractometer XRD 6000, Cu Kα radiation in the 2θ range of 10 - 70° at the scan speed of 0.1°/min.

For the electrical characterisation, BMT pyrochlore powder was cold pressed into a pellet of 8 mm in diameter and ~1.5 mm in thickness using a uniaxial hydraulic press. After sintering at 1075 °C for 24 h, the relative density above 90 % was obtained as which calculated from their geometrical and theoretical densities. The Au paste was used as electrodes and smeared on both sides of the pellet. The coated pellet was then dried and hardened in a muffle furnace by the programmed heating at 600 °C for 2 h. Impedance spectroscopy (IS) measurement in the low temperature range of 10–320 K was performed using an Agilent E4980A with Intelligent Temperature Controller (ITC 503S) while the high temperature range of 373–1073 K using a HP4192A impedance analyser. Both measurement sets covered the frequency range of 10 Hz - 1 MHz. IS data were modelled with various equivalent electrical circuits using $Z_{View}$ equivalent circuit fitting software.

## 3. Results and discussion

### 3.1. Experimental impedance data

The experimental details of phase purity and chemical stoichiometry of the prepared BMT pyrochlore, as confirmed by both XRD and elemental analyses could be found in our previous works [2,8,9]: (i) The phase-pure $Bi_{3.30}Mg_{1.88}Ta_{2.82}O_{13.88}$ pyrochlore belongs to a cubic symmetry with a space group of $Fd\,\overline{3}\,m$, (ii) The prepared composition forms part of the $Bi_{3+(5/2)x}Mg_{2x}Ta_{3-(3/2)x}O_{14-x}$ solid solution ($x = 0.12$) and the overall local electroneutrality is preserved through the proposed doping mechanism: 5/2 $Bi^{3+} \leftrightarrow Mg^{2+}$ + 3/2 $Ta^{5+}$ + $O^2$, (iii) The synthesis optimisation and the correct chemical stoichiometry are attainable wherein there is no systematic deviation of bismuth loss upon firing at high temperature and (iv) The pellet optimisation and all electrical data collection have been subjected to stringent procedure as found in Ref. [10].

Literally, pyrochlores and related phases in the BMT system have high bulk ε′ in the range of 73–84 and low tan δ, in the order of $10^{-4}$ - $10^{-3}$ at ~298 K [2,3,8,9,11]. $Bi_{3.30}Mg_{1.88}$ $Ta_{2.82}O_{13.88}$ exhibits ε′ of 74 at room temperature and 1 MHz, which is more than three-fold higher that the reported ε′ of 20 in $Bi_2MgTa_2O_9$ pyrochlore; however, tan δ of both systems are still reasonably low at ~0.002. Most authors also agreed that low ε′ with increasing tantalum content could be associated with the relatively lower polarisability of $TaO_6$ octahedra, if compared to that of $NbO_6$ in the other pyrochlores [4,7–11]. Similarly, higher tantalum content may lead to the problems of increased porosity and smaller average grain size. In other words, ε′ is negatively impacted due to the increased total surface area and poor connectivity between grains. Such findings are consistent with our previous works wherein lower ε′ are discernible in most of the studied Ta analogues [7–10]. To understand the low temperature electrical behaviour, BMT pyrochlore, $Bi_{3.30}Mg_{1.88}Ta_{2.82}O_{13.88}$ is chosen for the detailed impedance characterisation, as which reported earlier [8]. For four different fixed frequencies from 1 kHz to 1 MHz, the variation of ε′ as a function of temperature is plotted in the range of 20–320 K (Fig. 1a). The ε′ are frequency-independent above ~180 K, but show frequency dependency at all lower temperatures with a broad ε′ maximum that depends on both frequency and temperature. Upon cooling, maxima of dielectric constant, $\varepsilon'_{max}$ whose values of 78, 78, 77 and 77 are observed at the $T_m$ of 104 K, 120 K, 136 K and 154 K, respectively for 1 kHz, 10 kHz, 100 kHz and 1 MHz. In other words, the $T_m$ shifts to higher temperatures as the frequency increases. At temperatures below $T_m$, the magnitudes of $\varepsilon'_{max}$ values decrease with increasing frequency and this suggests a typical behaviour of relaxor ferroelectric. The relaxor behaviour is associated with a gradual transition from macroscopic paraelectric to a ferroelectric phase at a temperature below than that of the peak of ε' [2,4,5,12–15]. On the other hand, tan δ data over similar temperature and frequency ranges are shown in Fig. 1b. At temperatures above ~180 K, tan δ is too small to measure at any frequency in the range of $10^3$–$10^6$ Hz, thus portraying the insulating nature of the sample at higher temperatures. These data are taken together to show insulating dielectric behaviour at temperatures close to room temperature with the onset of frequency-dependent relaxor-like behaviour below ~180 K. The peak position at $T_m$ indicates the dynamic freezing temperature or glass like transition [12–15]. At temperatures above 180 K, the ε′ data are independent of frequency but there are dispersions can be seen below the $T_m$. Similar behaviour is also observed in the tan δ data. Thus, tan δ data (Fig. 1b) are both frequency- and temperature-dependent at temperatures below 180 K. The highest value of tan δ is 0.0214 at 1 kHz and $T_m$ of ~28 K and then, increases to 0.0306 at $T_m$ of ~64 K as the frequency increases up to 1 MHz.

A ferroelectric whose ε' values above the Curie temperature should follow the Curie-Weiss law (eq. (1)).

$$1/\varepsilon' = (T - T_0)/C \quad (1)$$

where $T_0$ is the Curie-Weiss temperature and C is the Curie-Weiss constant. The frequency-independent ε′ data above 154 K at fixed frequency of 1 MHz are used to fit the Curie-Weiss law (Fig. 2). The plots of inverse ε′ against temperature, T yield a linear slope and the extrapolated Curie temperature, $T_0$ value is found as ~ −4917 K. Similar approach is applied to ε′ data at different frequencies and this yields the values of −4765 K, −4739 K and −4761 K, respectively.

The dispersive characteristic of ε′ below $T_m$, as found in typical relaxor materials could be attributed to the formation of polar

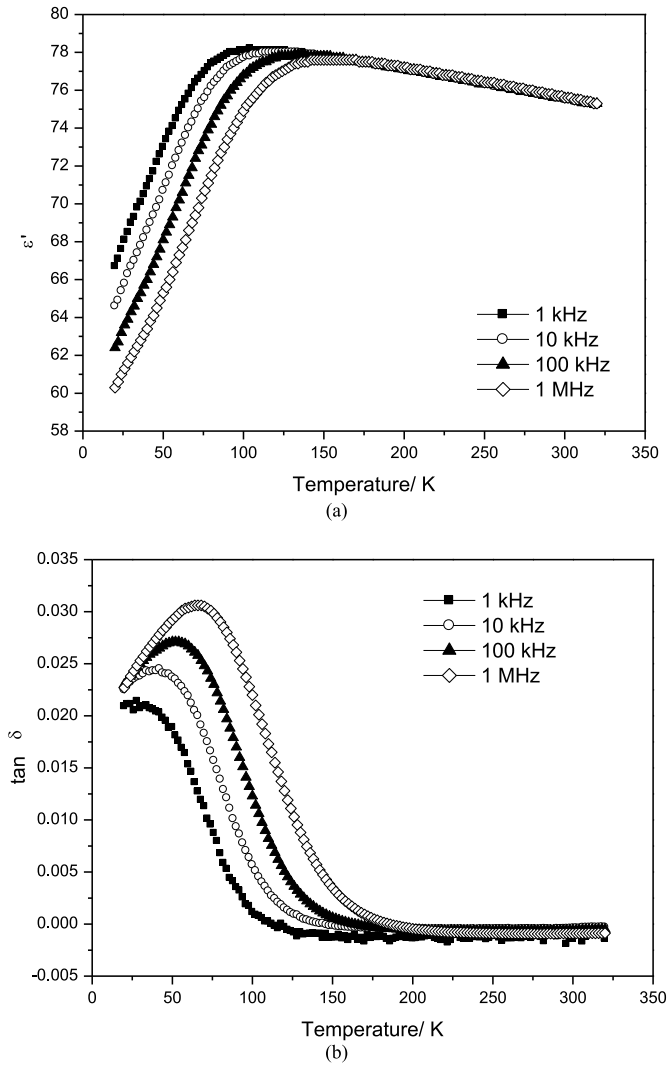


**Fig. 1.** (a) Dielectric constant, ε′ and (b) dielectric loss, tan δ of $Bi_{3.30}Mg_{1.88}Ta_{2.82}O_{13.88}$ pyrochlore at four fixed frequencies as a function of temperature in the temperature range of 20–320 K.

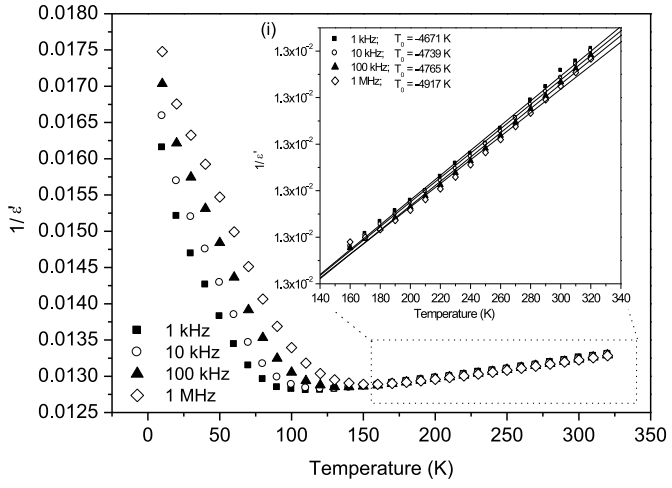


**Fig. 2.** The inverse of dielectric constant at four fixed frequencies as a function of temperature. The inset (i) indicates the experimental data of $Bi_{3.30}Mg_{1.88}Ta_{2.82}O_{13.88}$ pyrochlore fitting to the Curie-Weiss law.

nanodomains. The Burns temperature, $T_B$, on the other hand, is used to describe the onset of its formation for which the dispersion starts upon cooling [2,4,5]. Burns temperature was originally developed by Burns and Dacol [16] wherein the optic index of refraction of the ferroelectrics should follow a linear relation in high temperature region, except there was a possibility of departure from this linearity in low temperature region. As such, the starting temperature of this deviation was known as the Burns temperature, which was then used to describe the deviation of susceptibility from the Curie-Weiss law in lead magnesium niobate relaxor ferroelectrics [16]. The same concept was also extended to the study of $(Bi_{1.5}Zn_{0.5})(Nb_{0.5}Ti_{1.5})O_7$ relaxor ceramic [5], i.e. the temperature at which the ε' dispersion commences on cooling is often called the Burns temperature and may signify the onset of nanodomain formation. The Burns temperature can be recognised as the point above which the material behaves as a simple capacitor. The deviation between $T_m$ and $T_B$ could be calculated using eq. (2).

$$\Delta T_m = T_B - T_m \quad (2)$$

The $\Delta T_m$ of BMT pyrochlore at the frequencies of 1 kHz, 10 kHz, 100 kHz and 1 MHz are 48 K, 54 K, 58 K and 58 K, respectively. The deviation of $\Delta T_m$ implies that a diffuse phase transition (DPT) occurs in the sample. The DPT is a phenomenon at which a broaden ε' peak is observed against the temperature function. For a relaxor ferroelectric with DPT characteristic, a modified Curie-Weiss law is useful to describe the diffuse phase transition involved (eq. (3)).

$$(1/\varepsilon' - 1/\varepsilon_{max}) = (T - T_m)^{\gamma}/C \quad (3)$$

The diffuseness degree, γ of the BMT pyrochlore is determined using eq. (3) and the values are 1.43, 1.46, 1.31 and 1.62 at the frequencies of 1 kHz, 10 kHz, 100 kHz and 1 MHz, respectively (Fig. 3). These values imply that BMT pyrochlore is placed between a normal ferroelectric and an ideal relaxor ferroelectric where a diffuse phase transition occurs within the structure [14,15].

In a classical relaxor, a strong frequency dispersion is often portrayed by the low-temperature slope of its dielectric maximum. In order to characterise the dielectric constant peak, two relationships, either the Vogel-Fulcher equation could be used to analyse the frequency-dependence of $T_m$ relationship or by using the super exponential function. This behaviour is an analogy to the magnetic relaxation in spin-glass systems [14–18]. The Vogel-Fulcher equation takes the form as below [4,19].

$$f_m = f_0 \exp\left[-E_a/k(T_m - T_{vf})\right] \quad (4)$$

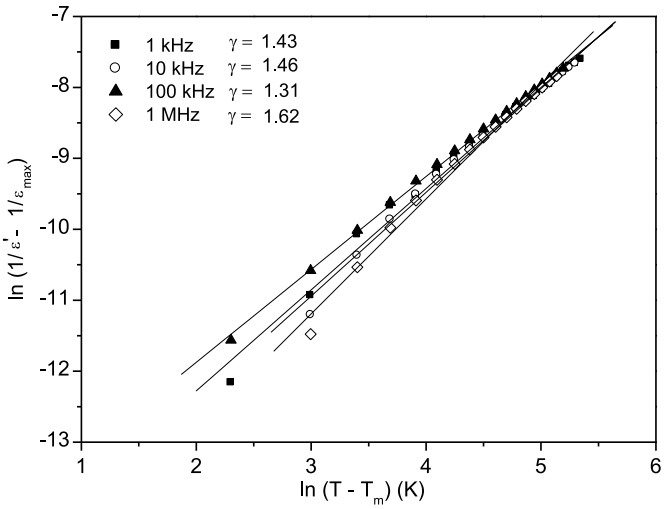


**Fig. 3.** $\ln(1/\varepsilon' - 1/\varepsilon_{max})$ against $\ln(T - T_m)$ of $Bi_{3.30}Mg_{1.88}Ta_{2.82}O_{13.88}$ pyrochlore at four fixed frequencies.

where k is Boltzmann's constant = 8.617 × $10^{-5}$ eV $K^{-1}$, $T_{vF}$ is the freezing temperature at which nanodomains is essentially frozen and $E_a$ is a measure of average activation energy. A Vogel-Fulcher fits to the $\varepsilon'_{max}$ is shown in Fig. 4 with the activation energy, $E_a$ value of 0.08 eV (inset of Fig. 4). Table 1 summarises the details of BMT pyrochlore concerning the temperature at which the maximum $\varepsilon'$ is obtained ($T_m$), $\varepsilon'$ maximum ($\varepsilon'_{max}$), diffuseness constant (γ), Curie-Weiss temperature ($T_0$) and Burns temperature ($T_B$) at different frequencies [4].

The capacitance, C′, data as a function of frequency are shown for a wide range of temperatures starting from 20 K to 1123 K (Fig. 5). At the lowest temperature of 20 K, the data show a power law response. With increasing temperature, curvatures are started to form at lower frequencies (Fig. 5a) and above the temperature of ~80 K, the low frequency data are almost plateau to give a frequency-independent capacitance (Fig. 5b and c). This frequency-independent C′ data stay until temperature of 573 K before strong dispersions are observed at low frequency with increasing temperature (Fig. 5e). Note that C' data are independent of frequency, but show decreasing values when the temperature increases from 180 K to 320 K (Fig. 5d).

Conductivity, Y′ data as a function of frequency of BMT pyrochlore are shown in the same temperature range (Fig. 6). At the lowest temperatures, the Y′ data show an almost linear power law response. With increasing temperature, the low frequency Y′ data show lower conductivity values and curvatures at the highest measurable temperatures, i.e., 150 and 160 K. The low frequency data appeared to show, again, a linear response with a slope of 2 on the log/log scale at temperature of ~20–50 K (Fig. 6a). Between 160 K and ~673 K, conductivities are too low to measure at any frequency. At higher temperatures, Y′ data show frequency-independent plateau with the onset of a dispersion at higher frequencies that disappears off scale at higher temperatures (Fig. 6b). These Y′ data confirm the insulating nature of the sample above ~160 K and show that only at very high temperatures, i.e., above 673 K, which possible to measure a dc conductivity of the samples. At temperatures below 160 K, the ac conductivity is clearly measurable but without any evidence for a limiting low frequency conductivity [2,4,5]. The conduction behaviour of the material obeys the Jonscher's universal power law [20].

$$\sigma_T(\omega) = \sigma(0) + \sigma_1(\omega) = \sigma_0 + A\omega^n \quad (5)$$

where σ(0) is the frequency independent dc conductivity, whereas $\sigma_1(\omega)$ is the frequency dispersive component of ac conductivity. The exponent n is between the value zero and one, i.e., n = 0 for dc conductivity and n

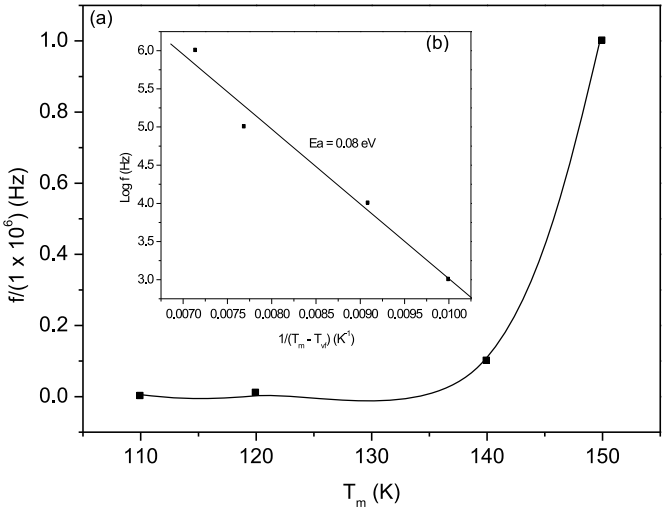


**Fig. 4.** Frequencies and temperatures of $\varepsilon'_{max}$ with fits to the Vogel-Fulcher equation, (a) $f_{max}$ as a function of $T_{max}$ and (b) Arrhenius plot of log $f_m$ as a function of $1/(T_m - T_{vf})$.

**Table 1**
The temperatures for which the dielectric constant maximum ($T_m$), dielectric constant maximum ($\varepsilon'_{max}$), diffuseness constant (γ), Curie-Weiss temperature ($T_0$) and Burns temperature ($T_B$) at four fixed frequencies.

| Frequency (Hz) | $T_0$ (K) | $T_B$(K) | $T_m$ (K) | $\varepsilon'_{max}$ | γ |
|---|---|---|---|---|---|
| 1 k | −4671 | 152 | 104 | 78 | 1.43 |
| 10 k | −4739 | 174 | 120 | 78 | 1.46 |
| 100 k | −4765 | 194 | 136 | 77 | 1.31 |
| 1 M | −4917 | 212 | 154 | 77 | 1.62 |

≤ 1 for ac conductivity. Value of n less than unity (n < 1) in BMT pyrochlore (Table 2) signifies that the ac conduction mechanism of the material involves sudden hopping process along with translational motion of the charge carriers [21,22].

### 3.2. Interpretation of impedance data and circuit modelling

Below room temperature, the impedance data show a combination of frequency-independent regions in both C′ and Y′ together with extensive regions where both parameters show frequency dispersions. At the lowest temperature, both C′ and Y' show an almost linear dependence on frequency scale at several temperatures, which is a characteristic of power law response and this suggests a Constant Phase Element (CPE), is required to fit the data [17–19,22–25]. The simple equivalent circuit, CPE is shown in Fig. 7a and expressed in the form below:

$$Y^* = A\omega^n + jB\omega^n \quad (6)$$

where ω = 2πf, f is the measuring frequency and j = √-1. Note that CPE, in the equivalent circuit analysis is often regarded as a circuit fitting parameter shows no physical significance; but is required to model departures from ideality in impedance data. It can be regarded as a combination of a frequency-dependent resistance, $A\omega^n$ in parallel with a frequency-dependent capacitance, $B\omega^n$. The parameters of CPE, either n, A and B are dramatic temperature dependent. The A and B are interrelated and the relative importance of the two components is given by the magnitude of the power law, n [18,19,22–24]. On logarithmic plots against frequency, therefore, Y′ data should fit a slope of n and C′ data should fit a slope of (n-1) since:

$$C^* = (j\omega C_0)^{-1} Y^* \text{ and } C' = BC_0^{-1}\omega^{n-1} \quad (7)$$

With increasing temperature, departure from the simple power law behaviour is seen in both C′ and Y′ data, which means that an additional circuit element is required to model the impedance response. At least part of this additional circuit element must be in series with the CPE, as otherwise it would not be possible to account for the departures from linearity seen in C′ and Y'. Alternatively, CPE is used to describe a capacitive process when a certain frequency dispersion present. CPE could be related to systems that show kind of self-scaling involving either (i) geometry origin that associated with fractal electrode or (ii) dynamic origin that linked with multiple trapping system [4,5].

Various equivalent circuits incorporating resistors and capacitors together with the CPE are tested in order to find a circuit(s) that best fitted the experimental data. We conclude that circuit Fig. 7b is the master circuit, which fits experimental data well over the temperature range of 110–130 K. At other temperatures, simplified versions of the circuit, obtained by eliminating one or more parameters, fit the data well. Thus, for temperatures below 110 K, resistance $R_2$ appears to be too large (Table 2) to have any significant role and the circuit therefore simplifies to Fig. 7c. Circuits in Fig. 7b and c have the series capacitance, $C_1$, which responsible for the low frequency departures from linearity in both Y′ and C′ plots. At the lowest temperature, 20 K, departures from linearity of Y′ and C' are barely distinguishable over the frequency range measured, therefore, elements $C_1$ and $C_2$ make little contribution to the impedance response at these temperatures. The circuit then simplifies to Fig. 7a.

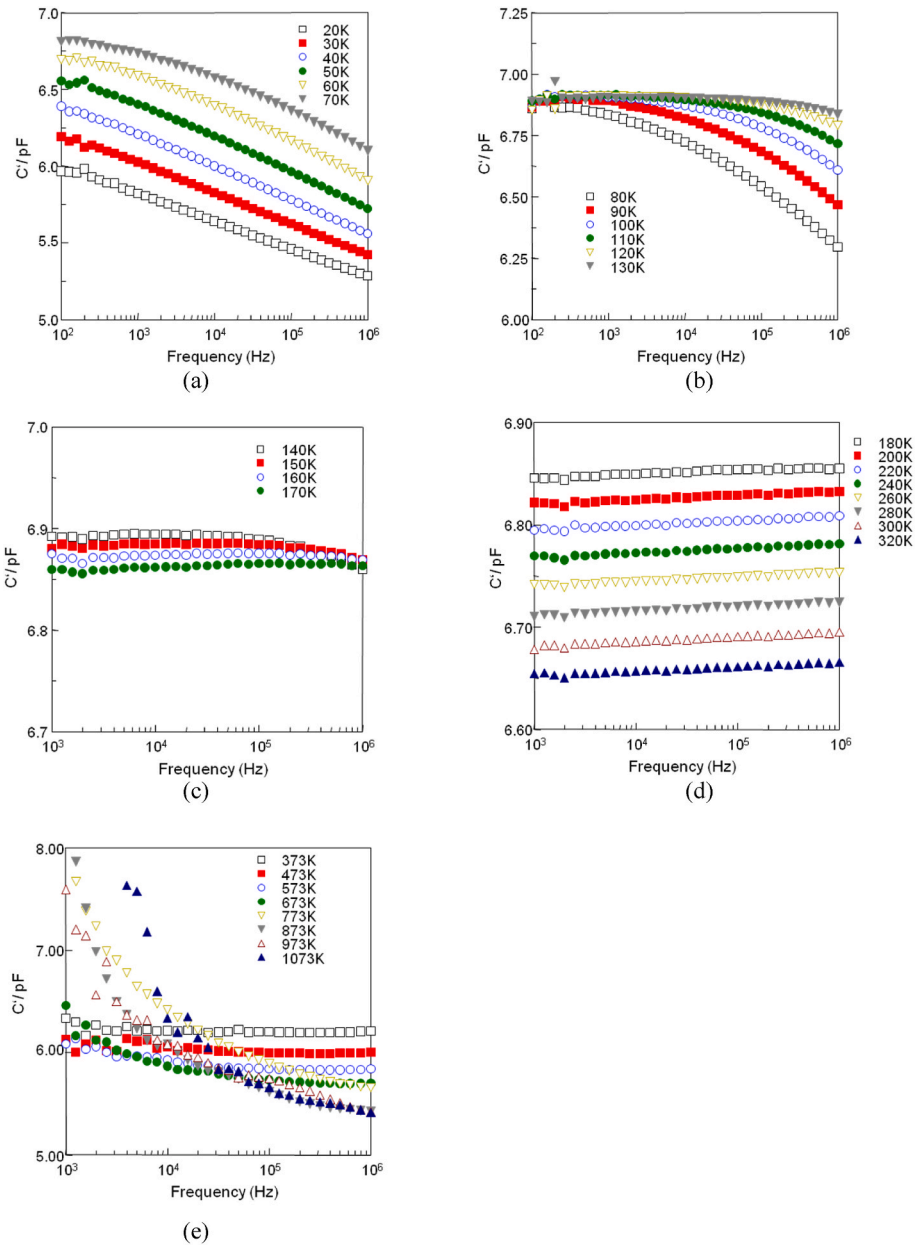


**Fig. 5.** Capacitance, C′ as a function of frequency for (a) 20–70 K, (b) 80–130 K, (c) 140–170 K, (d) 180–320 K and (e) 373–1073 K.

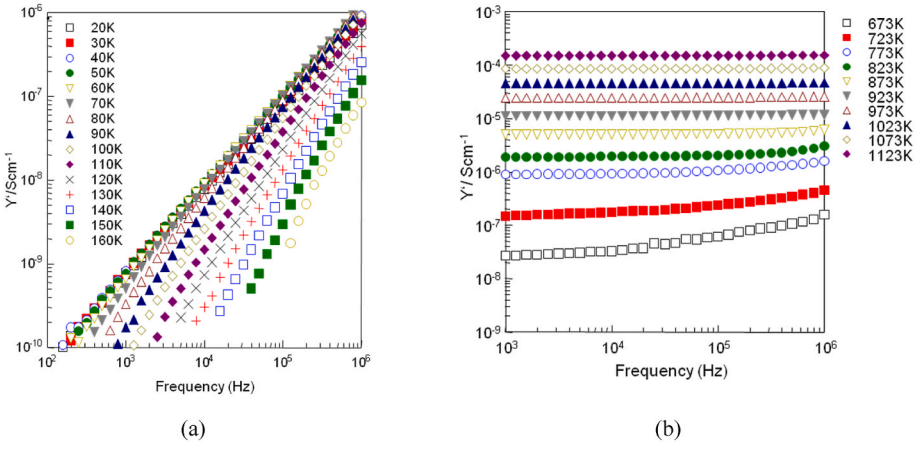


**Fig. 6.** Admittance, Y′ as a function of frequency for (a) 20–160 K and (b) 673–1123 K.

**Table 2**
Fitting data of $Bi_{3.30}Mg_{1.88}Ta_{2.82}O_{13.88}$ pyrochlore from 10 K to 320 K.

| Temperature (K) | $R_2$ (Ω cm) | $C_1$ (F $cm^{-1}$) × $10^{-12}$ | $C_2$ (F $cm^{-1}$) × $10^{-11}$ | A ($\Omega^{-1}cm^{-1}rad^{-1}$) | n |
|---|---|---|---|---|---|
| 10 | | 6.34 | 1.50 | $8.02 \times 10^{-11}$ | 0.86893 |
| 20 | | 6.89 | 1.19 | $7.62 \times 10^{-11}$ | 0.87544 |
| 30 | | 6.99 | 1.19 | $1.03 \times 10^{-10}$ | 0.86474 |
| 40 | | 7.04 | 1.22 | $1.47 \times 10^{-10}$ | 0.85158 |
| 50 | | 7.08 | 1.25 | $2.24 \times 10^{-10}$ | 0.83697 |
| 60 | | 7.03 | 1.45 | $4.75 \times 10^{-10}$ | 0.80452 |
| 70 | | 7.00 | 1.76 | $1.21 \times 10^{-09}$ | 0.76326 |
| 80 | | 6.97 | 2.24 | $3.80 \times 10^{-09}$ | 0.71220 |
| 90 | | 6.95 | 2.81 | $1.21 \times 10^{-08}$ | 0.66333 |
| 100 | | 6.93 | 4.19 | $5.88 \times 10^{-08}$ | 0.58782 |
| 110 | 29584 | 6.91 | 4.50 | $1.50 \times 10^{-07}$ | 0.56309 |
| 120 | 10327 | 6.91 | 5.80 | $4.45 \times 10^{-07}$ | 0.52390 |
| 130 | 2772 | 6.90 | 6.11 | $8.67 \times 10^{-07}$ | 0.51380 |
| 140 | 699.8 | 6.89 | | $5.40 \times 10^{-07}$ | 0.57719 |
| 150 | 221 | 6.89 | | $2.79 \times 10^{-07}$ | 0.64394 |
| 160 | | 6.87 | | | |
| 170 | | 6.86 | | | |
| 180 | | 6.85 | | | |
| 190 | | 6.84 | | | |
| 200 | | 6.83 | | | |
| 210 | | 6.81 | | | |
| 220 | | 6.80 | | | |
| 230 | | 6.79 | | | |
| 240 | | 6.77 | | | |
| 250 | | 6.76 | | | |
| 260 | | 6.75 | | | |
| 270 | | 6.73 | | | |
| 280 | | 6.72 | | | |
| 290 | | 6.70 | | | |
| 300 | | 6.69 | | | |
| 310 | | 6.67 | | | |
| 320 | | 6.66 | | | |

At temperatures above 130 K, $C_2$ becomes increasingly small and it becomes more difficult to refine satisfactorily a value for $C_2$; hence, circuit Fig. 7d is used. At still higher temperatures, above 150 K, the $CPE_2$ makes very little contribution to the impedance and $R_2$ becomes too small to have any significance at which point the equivalent circuit simplifies to a single capacitor, circuit Fig. 7e. Fits of experimental data to Y′ and C' are shown for four temperatures, 20, 100, 120, and 150 K (Fig. 8). Table 2 shows values of the various circuit parameters over the temperature range of 10–320 K. Data for 10 K are included although these are generally anomalous and do not fit in with the remaining trends.

Values for the various fitted parameters as a function of temperature are summarised in Fig. 9. Only $C_1$ could be fitted over almost the entire temperature range and its value ~6.66–7.08 pF $cm^{-1}$ (Fig. 9a) that correspond to a ε' of ~75–~80. In the temperature range of 110–130 K, a master circuit with a series capacitor, $C_1$ and parallel elements of $R_2$, $C_2$ and $CPE_2$ is used (Fig. 7b). $R_2$ is required to fit the data (Fig. 9b) and $R_2$ values decrease with increasing temperature (Fig. 9b). As mentioned earlier, resistance $R_2$ below 110 K appears to be too large to have any significant role at which these temperatures signify the domains become increasingly frozen, which make dipoles are more difficult to reorient [2,4,5]. Hence, the parameter $R_2$ could represent the difficulty of the cooperative displacements associated with nanodomains reorientation.

On the other hand, $C_1$ represents a series capacitance associated with relatively thick and insulating regions of the sample. In the temperature range of 160–320 K, a simple frequency-independent capacitor, $C_1$ whose values increase gradually with decreasing temperature and with bulk permittivity in the range of 75–77. At these temperatures, the material behaves as a simple capacitor (Fig. 7e). The $C_1$ data increase gradually with decreasing temperature from 320 to 50 K with corresponding bulk ε′ of 75–80. The $C_2$ data show a gradual increase above ~50 K and then decrease gradually below 50 K (Fig. 9a). This may be due to the relaxation behaviour in the sample. The high ε' values indicate considerable polarisation within the BMT lattice [2,4]. The magnitude of capacitance $C_1$ is small and shows very little temperature dependence (Table 2 and Fig. 9a). It is almost a frequency-independent capacitor which behaves as an ideal dielectric with no measurable conductivity. It is now clear that BMT is a perfect dielectric material at low temperatures since there is no evidence of any leakage conductivity, which would be represented by a finite resistance in parallel with the equivalent circuit, either element $C_1$ in Fig. 7 is a perfect blocking capacitor.

The capacitance, $C_2$ increases to maximum at the temperature of 130 K (Fig. 9a). Between the temperatures of 140–150 K, $C_2$ is too small and the polarisation process becomes tardier. In other words, the $C_2$ is very much temperature-dependent and the magnitudes of $C_2$ increase rapidly with the increasing temperature from an almost constant value of ~10 pF $cm^{-1}$ at the lowest temperature. However, the increment rate increases with temperature and $C_2$ value is too large to be determined above 140 K as $C_2$ value becomes difficult to refine (Fig. 9a). At temperature 160 K and above, the $C_2$ is not an identifiable parameter in the equivalent circuit and the material behaves as a simple capacitor.

### 3.3. Discussion

The BMT relaxor ferroelectric shows a Curie-Weiss law behaviour at the transition temperature, $T_c$, at which the peak does have a divergence but it is broad and rounded. This rounded peak position at $T_m$, indicates the dynamic freezing temperature or glass-like transition. On the other

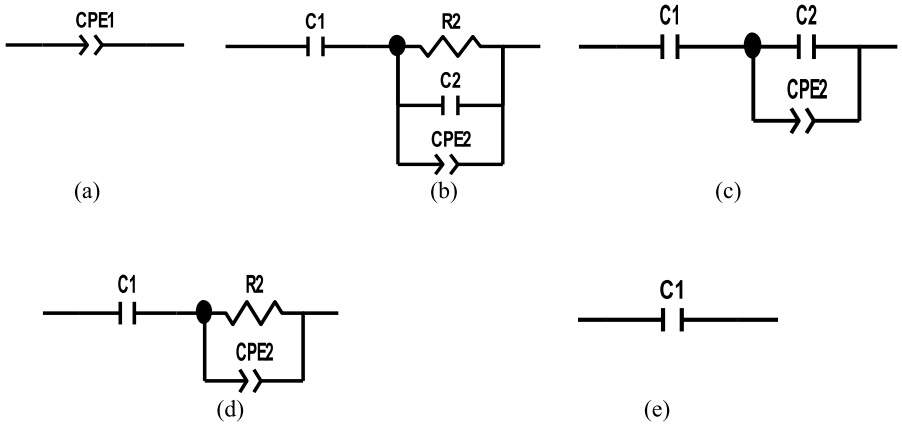


**Fig. 7.** Equivalent circuits showing different R, C, CPE combinations.

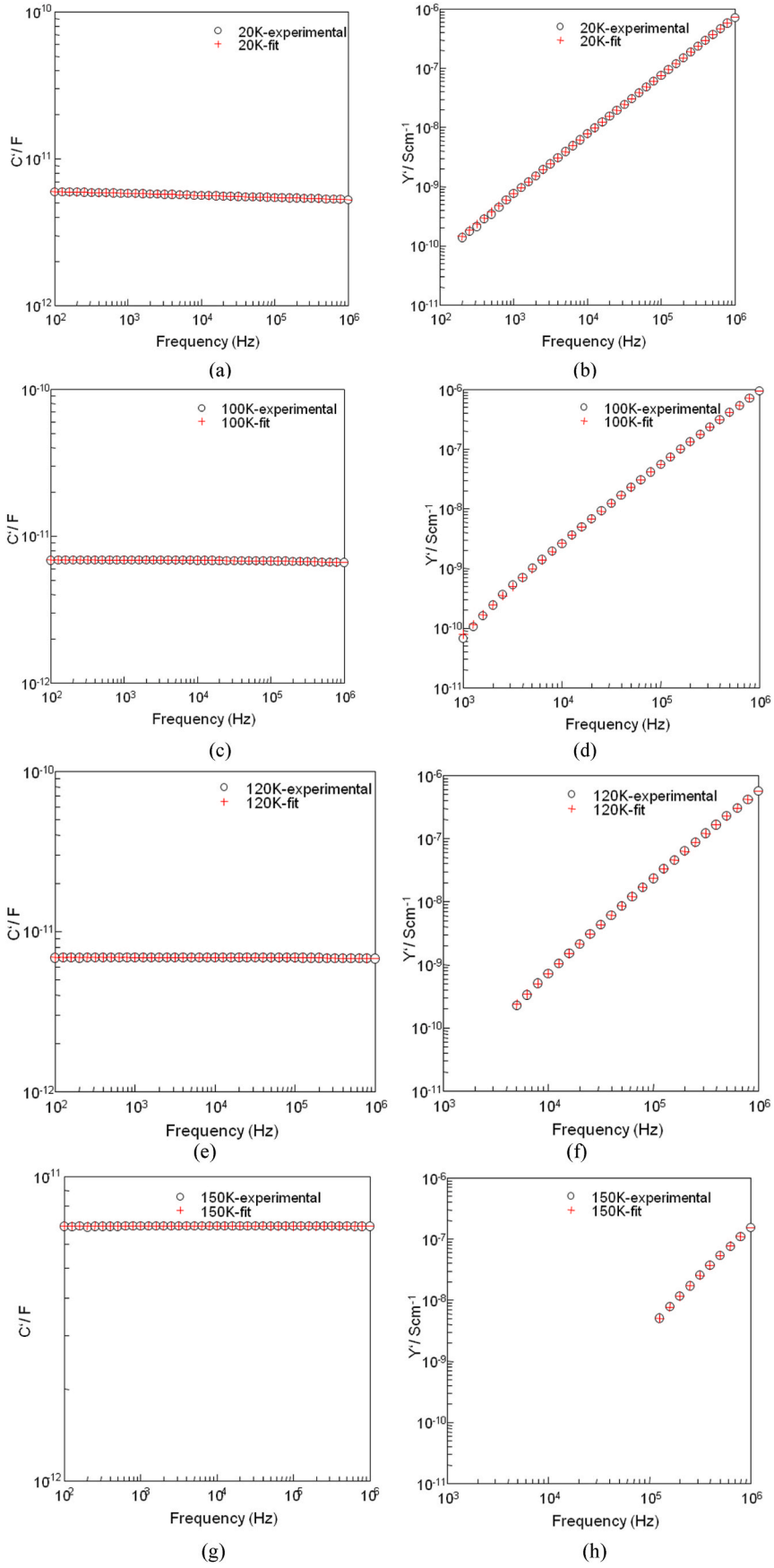


**Fig. 8.** Fit of the 20 K, 100 K, 120 K and 150 K data to circuit in Figs. 5 and 6.

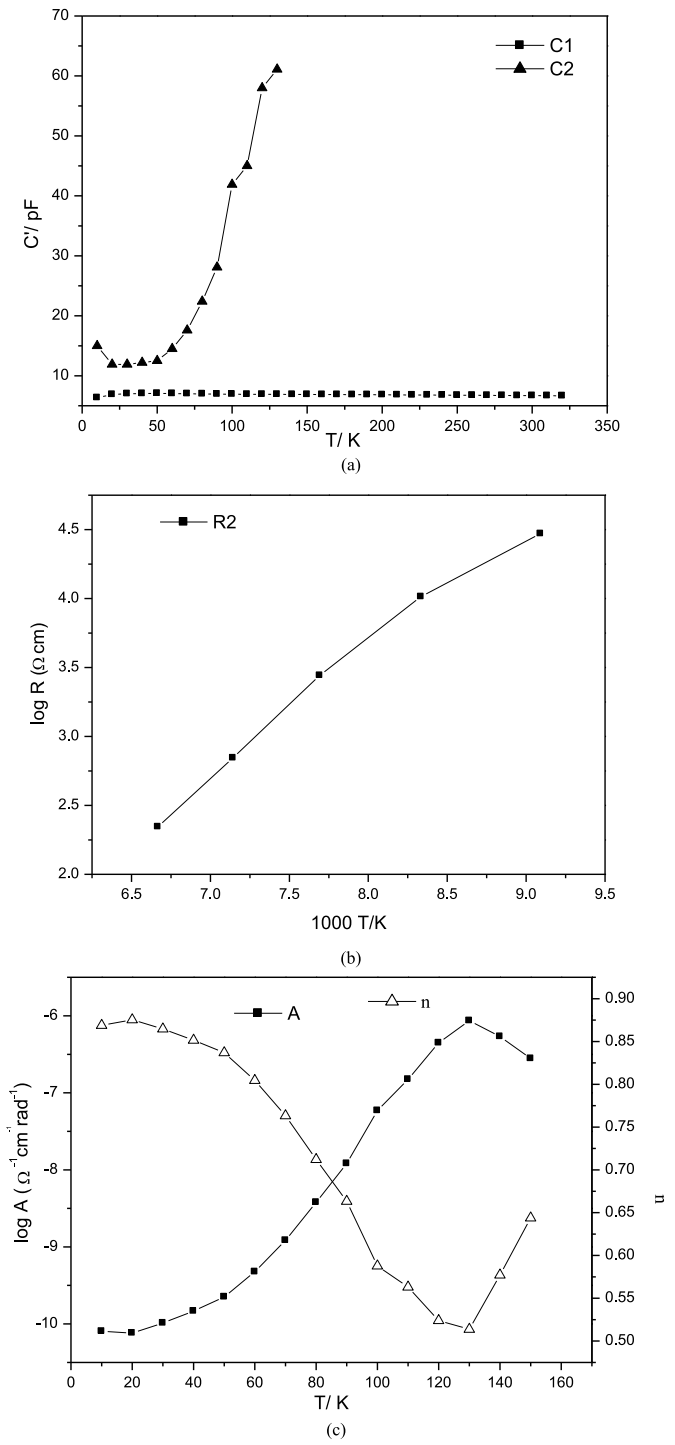


**Fig. 9.** Temperature dependence of (a) capacitance $C_1$ and $C_2$, (b) resistance $R_2$ and (c) $CPE_2$ and the n values.

hand, there is a strong frequency dispersion below peak position, $T_m$ where both $\varepsilon'$ and tan δ data are both frequency- and temperature-dependent in low temperature region (Fig. 1a and b) [4,5,12–14,17–19,23]. The dispersions seen in $\varepsilon'_{max}$ (Fig. 1a) are attributed to the existence of polar nanodomains within the crystal structure and this phenomenon provides evidence that the BMT pyrochlore is of a typical relaxor material. The polar regions in the crystal structure whose cooperative alignment is possible over only short distances. This is due to the frustration associated with chemical inhomogeneities, i.e., in the structure or the composition of the nanodomain regions. Considering the cationic occupancy in $Bi_{3.30}Mg_{1.88}Ta_{2.82}O_{13.88}$ pyrochlore, $Mg^{2+}$ ions are unequally distributed, i.e., at the eight coordinated A-site or six-coordinated B-site of the pyrochlore structure in accordance with the formula of $(Bi_{3.30}Mg_{0.70})(Mg_{1.18}Ta_{2.82})O_{13.88}$. This translates $Mg^{2+}$ has the site occupancies of 17.5 % and 29.5 % at the A-site and B-site, respectively. The A-site cations, $Bi^{3+}$ and $Mg^{2+}$, which have different requirements of ionic size and coordination environment while the B-site cations, $Mg^{2+}$ and $Ta^{5+}$, which also have similar criteria. Hence, the unusual and complicated structure could therefore the origin of the polarity and the formation of nanodomains [2,4,5].

On the other hand, the relaxation could be resulted from the hopping of dynamically disordered A-site cations and O′ ions among the closely spaced possible positions. The relative interaction between the cations at the disordered A-sites ($Mg^{2+}$ and $Bi^{3+}$) and the O' ions would form unstable dipoles within the pyrochlore structure [2,4,5]. Therefore, the dielectric relaxation is possibly formed due to the reorientation of the dipoles under external ac fields. Meanwhile, the inhomogeneous distribution of $Mg^{2+}$ in the pyrochlore structure also gives rise to additional random fields. This could yield multiwell potentials that have a wide distribution of heights, necessitating the different transition rates, for $Bi^{3+}$ and $Mg^{2+}$ cations. Such an interatomic potential can cause a broad dielectric relaxation [6,13,14,17–19,23]. This also agrees reasonably with the inclusion of CPE where the dynamical origin is involved.

In the relaxor-like BMT pyrochlore, $CPE_2$ is needed for the entire measuring temperatures except for temperatures higher than ~160 K. The value of n (Table 2) covers the entire temperature range of <160 K with the values from n → 1 at lowest temperatures correspond to a pure capacitor whereas n → 0 at higher temperatures corresponds to a pure resistor. This reveals the marked change in nature of the $CPE_2$ with temperature. The ac conductivity parameter, an increase by ~4 orders of magnitude within temperature range of 10–150 K (Table 2), this implies that the highly resistive nature of the $CPE_2$ at the lowest temperature is largely capacitive while increase in temperature, the $CPE_2$ is largely resistive [4]. In these temperature ranges, polar regions in the crystal structure, associated either with the A-sites containing Bi/Mg or the B-sites containing Mg/Ta start to generate a significant but small displacive or polarisation component that can respond to the ac measuring field. The magnitudes of the $CPE_2$ (A) parameter increase with increasing temperature from 30 K to 130 K (Fig. 9c–Table 2) but its magnitudes fall above temperature 130 K and onwards until 150 K. This is due to highly resistive of $CPE_2$ at high temperature while largely capacitive at lower temperatures. Considering the data and physical interpretations above, BMT pyrochlore is concluded to have similar relaxor behaviour like other pyrochlore analogues in the BZN, BZT, BZNT, BNN ternary systems [2,4,5,8–11,26]. Their relaxor electrical properties are intermediate between those of (i) first order ferroelectrics, which show sharp dielectric constant maxima as a function of temperature and (ii) dielectric materials, which show very little temperature dependence of dielectric constant.

## 4. Conclusion

$Bi_{3.30}Mg_{1.88}Ta_{2.82}O_{13.88}$ shows an interesting relaxor behaviour in the lower temperature range of 20–320 K over a wide frequency range from 10 Hz to 1 MHz. It achieves a dielectric constant maximum, $\varepsilon'_{max}$ of ~77 at the temperature of 154 K. The frequency-independent dielectric constant data above 154 K at fixed frequency of 1 MHz can be fitted with the Curie-Weiss law, while the relaxation features in $Bi_{3.30}Mg_{1.88}Ta_{2.82}O_{13.88}$ are well fitted with the Vogel-Fulcher equation. The equivalent circuit analysis shows an excellent method to present the impedance data involving temperature sweeps of $\varepsilon'$ and tan δ at fixed-frequency. The dielectric properties of $Bi_{3.30}Mg_{1.88}Ta_{2.82}O_{13.88}$ relaxor are satisfactorily modelled with different equivalent circuits at various temperatures.

## CRediT authorship contribution statement

**P.Y. Tan:** Formal analysis, Methodology, Writing – original draft, Investigation. **K.B. Tan:** Funding acquisition, Project administration, Resources, Supervision, Writing – original draft, Writing – review & editing. **C.C. Khaw:** Data curation, Formal analysis, Validation. **H.C. Ananda Murthy:** Software, Visualization, Writing – review & editing. **R. Balachandran:** Formal analysis, Software, Visualization. **S.K. Chen:** Investigation, Methodology, Supervision. **O.J. Lee:** Data curation, Formal analysis, Validation. **K.Y. Chan:** Resources, Software, Visualization, Writing – review & editing. **M. Lu:** Software, Validation, Visualization.

## Declaration of competing interest

The authors declare no competing interest for this work.

## Acknowledgement

Special thanks to the financial support (Fundamental Research Grant Scheme, 01-01-20-2304FR) from the Ministry of Higher Education, Malaysia. The authors also extend their gratitude to Prof. A.R. West for his technical advice and the low-temperature electrical data collection from the Department of Materials Science and Engineering, The University of Sheffield, UK.

## References

[1] F.A. Jusoh, K.B. Tan, Z. Zainal, S.K. Chen, C.C. Khaw, O.J. Lee, Novel pyrochlores in the $Bi_2O_3$-$Fe_2O_3$-$Ta_2O_5$ (BFT) ternary system: synthesis, structural and electrical properties, J. Mater. Res. Technol. 9 (2020) 11022–11034.
[2] P.Y. Tan, K.B. Tan, C.C. Khaw, Z. Zainal, S.K. Chen, O.J. Lee, M.P. Chon, Non-ferroelectric relaxor properties of BMN, $Bi_{3.55}Mg_{1.78}Nb_{2.67}O_{13.78}$ pyrochlore, J. Alloys Compd. 816 (2020) 152576.
[3] N.A. Zhuk, M.G. Krzhizhanovskaya, Thermal expansion of bismuth magnesium tantalate and niobate pyrochlores, Ceram. Int. 47 (2021) 30099–30105.
[4] R.A.M. Osman, N. Masó, A.R. West, Bismuth zinc niobate pyrochlore, a relaxor-like non-ferroelectric, J. Am. Ceram. Soc. 95 (2012) 296–302.
[5] R.A.M. Osman, A.R. West, Electrical characterization and equivalent circuit analysis of $(Bi_{1.5}Zn_{0.5})(Nb_{0.5}Ti_{1.5})O_7$ pyrochlore, a relaxor ceramic, J. Appl. Phys. 109 (2011) 074106.
[6] C. Ang, Z. Yu, H.J. Youn, C.A. Randall, A.S. Bhalla, L.E. Cross, J. Nino, M. Lanagan, Low-temperature dielectric relaxation in the pyrochlore $(Bi_{3/4}Zn_{1/4})_2(Zn_{1/4}Ta_{3/4})_2O_7$ compound, Appl. Phys. Lett. 80 (2002) 4807–4809.
[7] B.H. Nguyen, L. Norén, Y. Liu, R.L. Withers, X. Wei, M.M. Elcombe, The disordered structures and low temperature dielectric relaxation properties of two misplaced-displacive cubic pyrochlores found in the $Bi_2O_3$-$M^{II}O$-$Nb_2O_5$ (M = Mg and Ni) systems, J. Solid State Chem. 180 (2007) 2558–2565.
[8] P.Y. Tan, K.B. Tan, C.C. Khaw, Z. Zainal, S.K. Chen, M.P. Chon, Structural and electrical properties of bismuth magnesium tantalate pyrochlores, Ceram. Int. 38 (2012) 5401–5409.
[9] P.Y. Tan, K.B. Tan, C.C. Khaw, Z. Zainal, S.K. Chen, M.P. Chon, Phase equilibria and dielectric properties of $Bi_{3+(5/2)x}Mg_{2-x}Nb_{3-(3/2)x}O_{14-x}$ cubic pyrochlores, Ceram. Int. 40 (2014) 4237–4246.
[10] C.C. Khaw, K.B. Tan, C.K. Lee, A.R. West, Phase equilibria and electrical properties of pyrochlore and zirconolite phases in the $Bi_2O_3$-ZnO-$Ta_2O_5$ system, J. Eur. Ceram. Soc. (2012) 671–680.
[11] N.A. Zhuk, M.G. Krzhizhanovskaya, N.A. Sekushin, V.V. Kharton, B.A. Makeev, A. Belyy, R.I. Korolev, Dielectric performance of pyrochlore-type $Bi_2MgNb_{2-x}Ta_xO_9$ ceramics: the effects of tantalum doping, Ceram. Int. 47 (2021) 19424–19433.
[12] A.J. Bell, Calculations of dielectric properties from the super paraelectric model of relaxors, J. Phys. Condens. Matter 5 (1993) 8773–8792.
[13] G.A. Samara, The relaxational properties of compositionally disordered $ABO_3$ perovskites, J. Phys. Condens. Matter 15 (2003) R367–R411.
[14] X.G. Tang, K.H. Chew, H.L.W. Chan, Diffuse phase transition and dielectric tunability of $Ba(Zr_yTi_{1-y})O_3$ relaxor ferroelectric ceramics, Acta Mater. 52 (2004) 5177–5183.
[15] Y.H. Bing, A.A. Bokov, Z.G. Ye, Diffuse and sharp ferroelectric phase transitions in relaxors, Curr. Appl. Phys. 11 (2011) 514–521.
[16] G. Burns, F. Dacol, Crystalline ferroelectrics with glassy polarization behavior, Phys. Rev. B 28 (5) (1983) 2527.
[17] V. Dwight, S.J. Jang, L.E. Cross, M. Wuttig, Deviation from Curie-Weiss behavior in relaxor ferroelectrics, Phys. Rev. B 46 (1992) 8003.
[18] Z.Y. Cheng, R.S. Katiyar, X. Yao, A.S. Bhalla, Temperature dependence of the dielectric constant of relaxor ferroelectrics, Phys. Rev. B 57 (1998) 8166–8177.
[19] L.E. Cross, Relaxor ferroelectrics, Ferroelectrics 76 (1987) 241–267.
[20] A.K. Jonscher, The 'universal' dielectric response, Nature 267 (1977) 673–679.
[21] M. Tahir, S. Riaz, N. Ahmad, U. Khan, S. Atiq, M.A. Iqbal, S. Naseem, Anomalous dielectric behavior and correlation of barrier hopping mechanism with ferroelectricity in solvent assisted phase pure bismuth iron oxide nanoparticles, Mater. Res. Bull. 119 (2019) 110543.
[22] B.N. Parida, P.R. Das, R. Pahdee, R.N.P. Choudhary, Structural, dielectric and electrical properties of $Li_2Pb_2La_2W_2Ti_4Nb_4O_{30}$ ceramic, Bull. Mater. Sci. 36 (2013) 883–892.
[23] S. Kamba, V. Porokhonskyy, A. Pashkin, V. Bovtun, J. Petzelt, Anomalous broad dielectric relaxation in $Bi_{1.5}Zn_{1.0}Nb_{1.5}O_7$ pyrochlore, Phys. Rev. B 66 (2002) 054106.
[24] A.R. West, D.C. Sinclair, N. Hirose, Characterization of electrical materials, especially ferroelectrics, by impedance spectroscopy, J. Electroceram. 1 (1997) 65–71.
[25] M.A. Hernandez, N. Maso, A.R. West, On the correct choice of equivalent circuit for fitting bulk impedance data of ionic/electronic conductors, Appl. Phys. Lett. 108 (2016) 152901.
[26] J.C. Nino, M.T. Lanagan, C.T. Randall, Dielectric relaxation in $Bi_2O_3$-ZnO-$Nb_2O_5$ cubic pyrochlore, J. Appl. Phys. 89 (2001) 4512–4516.